Broadband Electroabsorption Modulators Design Based on Epsilon-Near-Zero Indium Tin Oxide

Hongwei Zhao, Yu Wang, Antonio Capretti, Luca Dal Negro, and Jonathan Klamkin, *Senior Member, IEEE*

***Abstract*—In this paper, we propose a compact silicon (Si) electroabsorption modulator based on a slot waveguide with epsilon-near-zero indium tin oxide materials. In order to integrate the device with low-loss Si strip waveguides, both butt-coupling and evanescent-coupling schemes are investigated. For both cases, our electroabsorption modulator demonstrates a high extinction ratio and a low insertion loss over a wide optical bandwidth.**

***Index Terms*—Integrated optoelectronics, optical modulators, plasmonics.**

I. Introduction

As AN integration platform, silicon (Si) photonics can demonstrate single-chip, CMOS-compatible photonic integrated circuits for optical interconnect applications [1]–[3]. Significant development has been carried out in realizing low-loss waveguides, germanium (Ge)-on-Si photodetectors, and Si optical modulators based on p-n junctions. Conventional Mach–Zenhder modulators, however, suffer from low efficiency, high insertion loss (IL), and large footprint [4]. By utilizing a microring resonator, the footprint can be significantly reduced, but such devices exhibit narrow optical bandwidth and thermal instability [5]. Electro-absorption modulators based on tensile-strained Ge quantum wells or bulk Ge/Si materials are promising, however require sophisticated epitaxial growth [6], [7].

Recently, CMOS-compatible transparent conducting oxides (TCOs) [e.g., indium tin oxide (ITO), aluminum zinc oxide, and gallium zinc oxide] have shown promise for integrated electro-absorptionmodulators [8]–[12]. The permittivity of TCOs can be tuned by actively adjusting the carrier density, therefore these materials respond to applied electric signals with absorption modulation. The modulation speed is limited only by the *RC* delay. The ITO modulator based on high-confined hybrid plasmon waveguides has demonstrated an extinction ratio (ER) of 5 dB with a 5-μm device length at the wavelength of 1.31 μm; and it can be further improved to be 6.0 $\mathrm{dB}\mu\mathrm{m}^{-1}$ [13], [14]. When the permittivity of the ITO material is tuned to be around zero, which is referred as the “epsilon-near-zero” (ENZ) state, the corresponding absorption loss can be optimized, enabling a higher ER. A previous reported electro-absorption modulator with “ENZ” ITO has shown a 3-dB ER with a 27-μm long device at the wavelength of 1.55 μm [15]. In their work, the ITO layer along with a thin $\mathrm{HfO_2}$ layer are deposited on top of a Si strip waveguide, which provides a small optical confinement inside the active ITO material thus limits the device performance.

In this work, we propose a high-confinement Si slot-waveguide modulator design based on engineered ENZ ITO materials. First, we characterize ITO films with different carrier concentrations and use the experimentally extracted parameters in electromagnetic simulations to design a modulator structure. Then, we investigate both butt coupling and evanescent coupling of the proposed device with conventional Si strip waveguides. In both coupling schemes, the compact electro-absorption modulators designs, with device length $\leq$1.5 μm, demonstrate a high ER over a wide optical bandwidth while maintaining relatively low IL.

This paper is organized as follows. In Section II, the measured permittivity of the ITO samples and the corresponding “ENZ” states are discussed. The absorption study based on a 2-D mode solver is presented in Section III. In Section IV, we propose a butt-coupled scheme with polarization rotators connecting the Si strip waveguides and the ITO modulator. The conventional evanescent coupling is also investigated. At last, Section V concludes this work.

II. Material Synthesis and Characterization

The permittivity of the ITO films is described by the Drude model [15]:

$$\varepsilon = \varepsilon_r + j\varepsilon_i = \varepsilon_\infty - \frac{\omega_p^2}{\omega(\omega + j\gamma)} \tag{1}$$

where the plasma frequency, ω_p, is given by $\omega_p^2 = Ne^2/\varepsilon_0 m^*$, ε_∞ is the high-frequency permittivity, γ is the electron scattering rate, N is the free-carrier concentration in the material, and m^* is the effective mass of the electron. According to (1), the permittivity of ITO can be tuned by actively changing the carrier concentration. With such an ITO layer embedded in a dielectric waveguide, the light absorption can be modulated accordingly.

ITO samples were prepared by radio-frequency magnetron sputtering (Denton Discovery 18) on Si substrates from an ITO (99.99%) disc target of 4 in in diameter. The ITO target power was 200 W, and post-deposition annealing treatments were applied to tune the optical dispersion of the films.

Manuscript received October 1, 2014; revised November 14, 2014; accepted November 15, 2014. Date of publication November 26, 2014; date of current version January 7, 2015. This work was supported in part by the Boston University College of Engineering Dean’s Catalyst Award and the AFOSR Program “Emitters for high density information processing using photonic-plasmonic coupling in coaxial nanopillars” under Award FA9550-13-1-0011. H. Zhao and Y. Wang equally contributed to this work.

H. Zhao, Y. Wang, and A. Capretti are with the Department of Electrical and Computer Engineering, Boston University, Boston, MA 02215 USA (e-mail: hwzhao@bu.edu; yuwang01@bu.edu; capretti@bu.edu).

L. D. Negro and J. Klamkin are with the Department of Electrical and Computer Engineering and also with the Department of Material Science and Engineering, Boston University, Boston, MA 02215 USA (e-mail: dalnegro@bu.edu; klamkin@bu.edu).

Color versions of one or more of the figures in this paper are available online at http://ieeexplore.ieee.org.

Digital Object Identifier 10.1109/JSTQE.2014.2375153

1077-260X © 2014 IEEE. Translations and content mining are permitted for academic research only. Personal use is also permitted, but republication/redistribution requires IEEE permission. See http://www.ieee.org/publications_standards/publications/rights/index.html for more information.

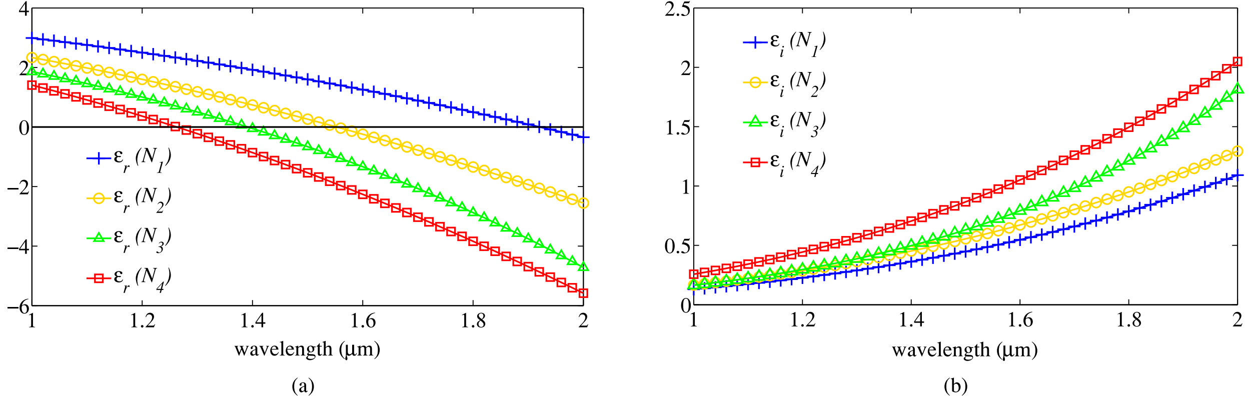

Fig. 1. Permittivity of ITO with different carrier concentrations ($N_1 = 4.33 \times 10^{20}$ cm^{-3}, $N_2 = 6.67 \times 10^{20}$ cm^{-3}, $N_3 = 8.31 \times 10^{20}$ cm^{-3} and $N_4 = 9.58 \times 10^{20}$ cm^{-3}), measured by spectroscopic ellipsometry. The thickness of ITO in the tested samples is 35 nm. (a) the real part of the complex permittivity; (b) the imaginary part of the complex permittivity.

The permittivity was directly measured using spectroscopic ellipsometry (Woollam VASE) [17]. The measured permittivity of ITO with different carrier concentrations (extracted from the measured plasma frequency), are shown in Fig. 1. For the ITO samples with carrier concentrations from N_1 to N_4, the ENZ wavelengths, are 1920, 1550, 1390 and 1270 nm, respectively.

With the above measurements, we have demonstrated that the ENZ wavelength of ITO can be shifted into the near infrared regime with a carrier concentration of $\sim 10^{20}$ cm^{-3}. Recent works by E. Feigenbaum etc., [16] on the ITO material have experimentally demonstrated that the change of the carrier concentration inside the thin ITO layer (ΔN) up to 10^{22} cm^{-3} can be achieved by carrier accumulation at the ITO/oxide interface under a few volts applied across the metal/oxide/ITO structure. Therefore, the permittivity of the ITO layer would be tunable by adjusting the applied voltage. In the next section, we will use the measured permittivity of ITO to design electro-absorption modulators embedded with ENZ ITO materials.

III. Mode Analysis and Modulator Design

Fig. 2(a) shows the cross-section schematic of our proposed slot-waveguide modulator based on ITO. The structure consists of a Si strip waveguide (of thickness $t_1 = 220$ nm) on a buried oxide layer, an active ITO layer as thin as $t_{\mathrm{ITO}} = 10$ nm (as demonstrated by [14]), two thin silicon dioxide (SiO_2) buffer layers ($t_b = 10$ nm) and a poly-Si capping layer ($t_2 = 160$ nm). The width of the modulator is 500 nm. The optical intensity of the TM modes is well confined in the slot, which effectively enhances the overlap of the optical modes and the ITO active medium. Some previous experimental work [13], [16] have already demonstrated that a suitable voltage applied across the metal/SiO_2/ITO structure allows to tune the permittivity of the ITO layer by carrier accumulation at the ITO/SiO_2 interface, thereby varying the optical loss of the modulator structure. The carrier concentration layer at the ITO/SiO_2 has been estimated to be 5 ± 1 nm thick. Accordingly, we will assume that a 5-nm thick accumulation layer can be electrically controlled in the ITO at the interface with SiO_2, and that the permittivity can be tuned by an applied voltage.

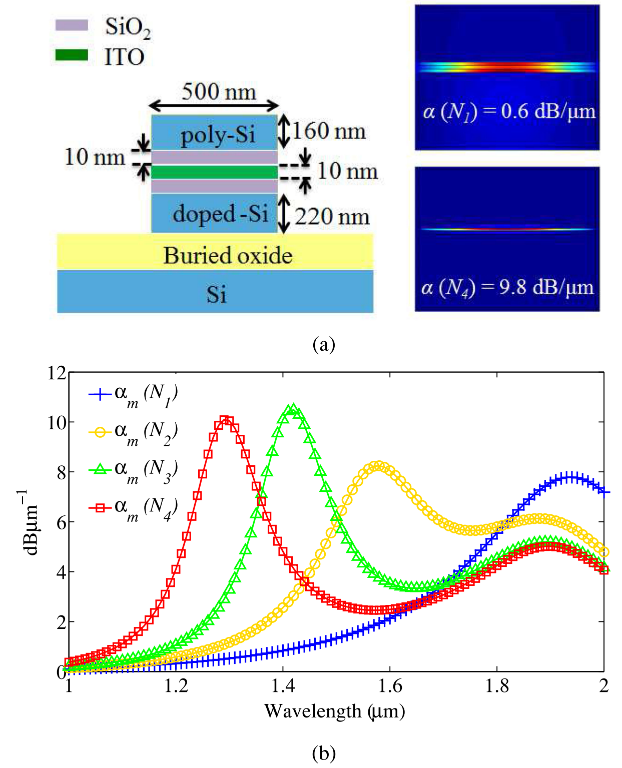

Fig. 2. (a) Schematic of the modulator structure and the profiles of the fundamental TM mode ($\lambda = 1310$ nm); (b) modulator absorption loss for different carrier concentrations based on a 2-D FDTD mode solver analysis.

The optical loss of the fundamental TM mode (α_m) of the slot-waveguide modulator is primarily due to the free-carrier absorption in the active ITO layer. This loss can be approximated by the product of the optical mode confinement factor (Γ) and the material absorption of the bulk ITO (α_b):

$$\alpha_m = \Gamma \cdot \alpha_b \tag{2}$$

where $\alpha_b = 2k_0 \cdot \mathrm{Im}[\varepsilon^{1/2}]$. The confinement factor, Γ, depends on $|\varepsilon|$ and the waveguide structure (the active layer thickness, the buffer material and thickness) [15]. As the permittivity is tuned to induce absorption modulation, both Γ and α_b are altered.

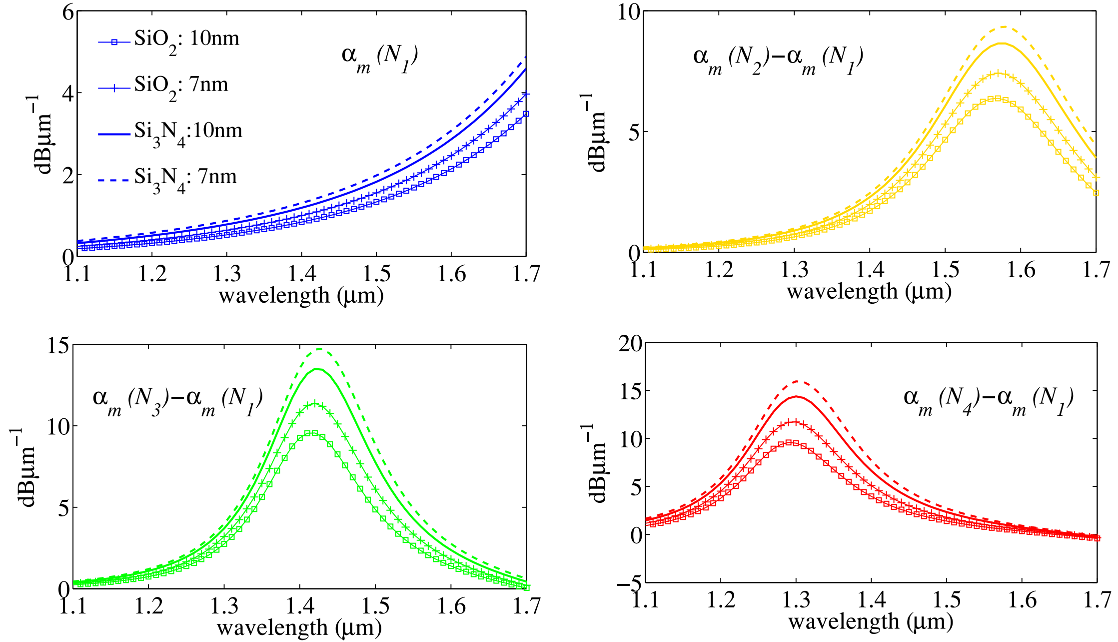

Fig. 3. Modulator performance with different buffer materials and thicknesses.

A smaller $|\varepsilon|$ can enhance the electric field (E) magnitude confined in the ITO layer due to the continuity of the normal component of the electric displacement field ($D = \varepsilon E$). Therefore, it is important to engineer the ENZ condition so that a minimum $|\varepsilon|$ is achieved for a state with high optical loss. As shown in Fig. 2(a), the electrical intensity of the fundamental TM mode is confined in the SiO_2/ITO/SiO_2 slot with ITO of $N_1 = 4.33 \times 10^{20}$ cm^{-3} , resulting in a small absorption loss (0.6 dB/μm^{-1}) at the wavelength of 1.31 μm. When the carrier concentration is tuned to be $N_4 = 9.58 \times 10^{20}$cm^{-3}, the ϵ_r of the ITO is near zero. The electrical intensity is mostly confined only in the ENZ ITO material, thus a high absorption loss (9.8 dB/μm^{-1}) is obtained at this state.

Utilizing the permittivity results of the ITO in Section II, we employ a 2-D mode solver to simulate the optical loss of the fundamental TM mode (TM_0) of the modulator. Fig. 2(b) shows the optical loss of the TM_0 mode of the slot-waveguide structure with ITO carrier concentration $N_1 = 4.33 \times 10^{20}$ cm^{-3}, $N_2 = 6.67 \times 10^{20}$ cm^{-3}, $N_3 = 8.31 \times 10^{20}$ cm^{-3}, and $N_4 = 9.58 \times 10^{20}$ cm^{-3}. Over the entire optical fiber communications band, the mode absorption loss (α_m) is fairly low for a carrier concentration of N_1, and is relatively high for carrier concentrations of N_2 , N_3, and N_4. Therefore, we define the state with carrier concentration N_1 as the ON state. As shown in Fig. 2(b), the maximum optical loss for N_2, N_3 and N_4 are achieved at 1.58 , 1.42, and 1.29 μm, respectively. Then, we can optimize the OFF state of the modulator for different wavelengths of operation. The performance of the electro-absorption modulator is then determined by the ratio of the optical loss in the ON state and OFF state where:

$$\alpha_{\rm ON} = \alpha_m(N_1) \tag{3}$$

$$\Delta\alpha = \alpha_m(N_i) - \alpha_m(N_1) \quad (i = 2, 3, 4). \tag{4}$$

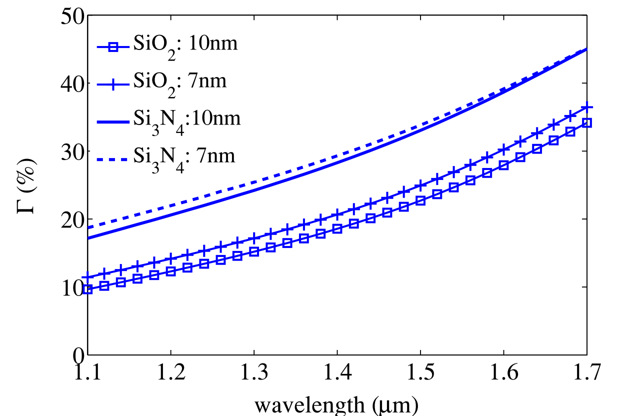

Fig. 4. The optical confinement factor (Γ) inside the ITO layer with a carrier concentration of $N_1 = 4.33 \times 10^{20}$ cm^{-3}.

For the slot-waveguide structure, Γ depends on the buffer layer thickness and its refractive index. Therefore, we evaluate the performance of the modulator with two different process compatible buffer materials, SiO_2 and silicon nitride (Si_3N_4), and two different buffer thicknesses, 10 and 7 nm. The corresponding $\alpha_{\rm ON}$ and $\Delta\alpha$ are plotted in Fig. 3. The modulator with 10-nm thick SiO_2 buffers demonstrates the minimum $\alpha_{\rm ON}$, which is only 0.55 dBμm^{-1} at the wavelength of 1.31 μm, and 1.68 dBμm^{-1} at the wavelength of 1.55 μm. The maximum $\Delta\alpha$ is achieved with 7-nm thick Si_3N_4 buffers: 15.9 dBμm^{-1} at 1.31 μm (for carrier concentration increased from N_1 to N_4) and 8.9 dBμm^{-1} at 1.55 μm (for carrier concentration increased from N_1 to N_2). Fig. 4 demonstrates the optical confinement factor (Γ) inside the active ITO layer with a carrier concentration of $N_1 = 4.33 \times 10^{20}$ cm^{-3}. Generally, with the same thickness, the structure with the Si_3N_4 buffer shows higher $\alpha_{\rm ON}$ as well as higher $\Delta\alpha$ since it enables a higher Γ. For a given

buffer material, the 10-nm thickness shows lower $\alpha_{\rm ON}$ and lower $\Delta\alpha$ due to a smaller Γ.

For a specific application and wavelength of interest, several parameters such as the carrier concentration for the OFF state, and the material and thickness of the dielectric buffers should be selected accordingly. For instance, if the target operating wavelength is 1.31 μm, then a modulator with 7-nm thick $\rm Si_3N_4$ buffers and carrier concentration tuning from N_1 to N_4 would be preferred. These conditions enable a maximum $\Delta\alpha$ while $\alpha_{\rm ON}$ is only 0.9 dBμm^{-1} at this wavelength. If the modulator is designed to work at the wavelength of 1.55 μm, then maintaining a low $\alpha_{\rm ON}$ is an important consideration since the absorption loss increases as the wavelength increases. Based on the previous experimental results and analysis in [13] and [16], the bias voltage for our proposed modulator is estimated to be 2–4 V, which depends on the oxide buffer (its refractive index n_b and thickness t_b) and the carrier concentration change (ΔN). In a future work, the required bias voltage will be studied through ellipsometry and optical transmission measurements after fabricating the proposed geometry and making contacts on the ITO and doped-Si layer.

IV. Integration of Slot-Waveguide Modulator With Si Strip Waveguides

In this section, we present two methods to integrate the ITO modulator with conventional Si strip waveguides. First, we propose a butt-coupled scheme with polarization rotators connecting the TE-loaded Si waveguides and the TM-mode slot-waveguide modulator (1-μm device length) section. This scheme works well for a wide optical band: from 1.28 to 1.60 μm by choosing suitable carrier concentrations. Second, the evanescent-coupling scheme is presented at the wavelength of 1.31 μm.

A. Butt-Coupled Scheme

For on-chip optical interconnects, the proposed compact and efficient electro-absorption modulator should be integrated with Si strip waveguides in the Si-on-insulator platform since these waveguides exhibit low propagation and bend loss. Based on mode analysis, the optical loss of the $\rm TM_0$ mode of the slot-waveguide modulator is efficiently modulated by tuning the carrier concentration in the active ITO layer. Therefore, it is critical to optimize the coupling efficiency (η) from the Si strip waveguides to the $\rm TM_0$ mode of the slot-waveguide modulator [18].

Fig. 5 shows a 3-D schematic diagram of the proposed slot-waveguide modulator butt coupled to low-loss Si strip waveguides. Here, the dielectric buffers are 7-nm thick $\rm Si_3N_4$ layers. In such a 3-D structure, the total propagation loss depends on the modal loss (α_m) and the coupling efficiency (η) from the strip waveguide to the slot waveguide. The modulator performance is given by the IL and the ER:

$$\mathrm{IL} = 10\log\left[\frac{\mathrm{I_{in}}}{\mathrm{I_{out}(N_1)}}\right] \tag{5}$$

$$\mathrm{ER} = 10\log\left[\frac{\mathrm{I_{out}(N_1)}}{\mathrm{I_{out}(N_i)}}\right] \quad (\mathrm{i} = 2, 3, 4). \tag{6}$$

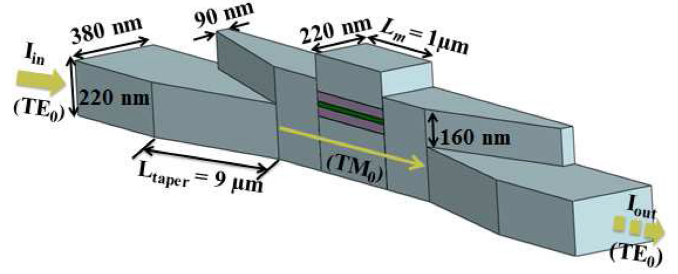

Fig. 5. Three-dimensional schematic of the slot-waveguide modulator (with 7-nm thick $\rm Si_3N_4$ buffers) butt coupled to Si strip waveguides.

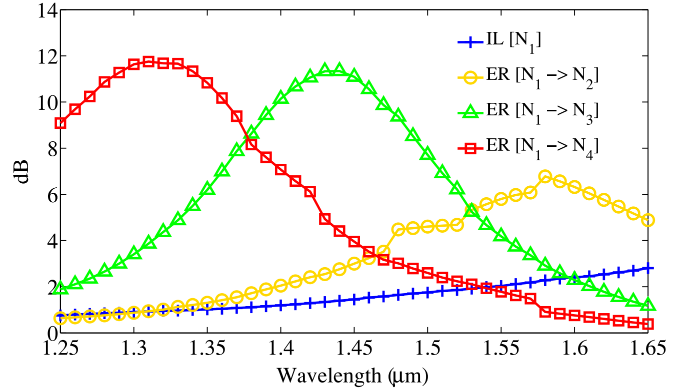

Fig. 6. The modulator performance of the butt-coupled structure (1.0-μm modulator length) with the carrier concentration tuned from N_1 to N_2, N_1 to N_3 and N_1 to N_4, respectively.

At the input, the horizontal Si strip waveguide is 220 nm thick and 380 nm wide, which is designed for single mode operation. The fundamental TE mode ($\rm TE_0$) is launched in the horizontal Si strip waveguide, then converted to the $\rm TM_0$ mode through a polarization rotator [18], [19]. The polarization rotator consists of two vertically stacked linear width tapers (9 μm in length). The end of the polarization rotator connects to a vertical strip waveguide (380 nm thick and 220 nm wide). The resulting $\rm TM_0$ mode of the vertical strip waveguide is then coupled to the $\rm TM_0$ mode of the slot-waveguide modulator. The modulator length L_m is only 1 μm for this design. Following propagation in the modulation region, the light is coupled to the $\rm TM_0$ mode of a strip waveguide and then rotated back to the $\rm TE_0$ strip mode through the output rotator.

A 3-D FDTD simulation tool is employed to further evaluate the performance of the ITO-based Si modulators. Fig. 6 shows the modulator performance when the carrier concentration is tuned from N_1 to N_2, N_1 to N_3 and N_1 to N_4, respectively. For a wavelength range from 1.53 to 1.64 μm, the ER is greater than 5 dB while the IL is less than 2.7 dB when the carrier concentration is tuned from N_1 to N_2. At 1.55 μm, the ER and IL are 5.8 and 2.0 dB, respectively. If the 7-nm thick $\rm Si_3N_4$ buffers are replaced by some 10-nm thick $\rm SiO_2$ buffers, the IL can be further reduced. When the carrier concentration is tuned from N_1 to N_4, the ER is greater than 6.0 dB while the IL is less than 1.3 dB for a wavelength range from

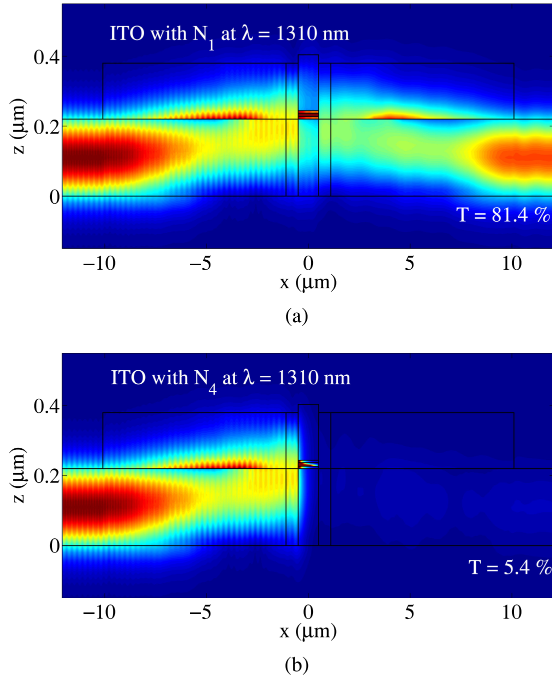

Fig. 7. The light propagating from the front end to the back end in the butt-couple scheme at $\lambda = 1.31$ μm: (a) $N = N_1$; (b) $N = N_4$.

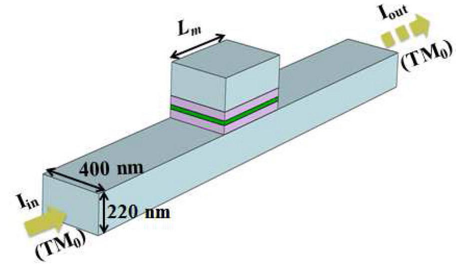

Fig. 8. Three-dimensional schematic of the slot-waveguide modulator (with 10-nm thick SiO_2 buffers) evanescently coupled to Si strip waveguides.

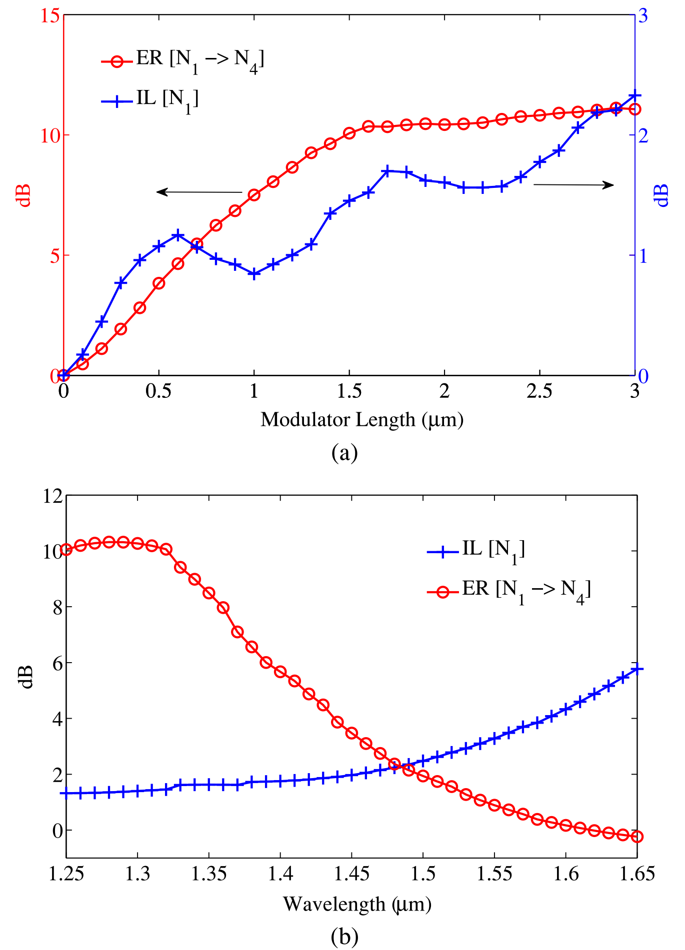

Fig. 9. (a) ER and IL versus modulator length (L_m) at 1.31-μm wavelength in the evanescent-coupled scheme; (b) modulator performance with L_m = 1.5 μm for a wavelength range from 1.25 to 1.65 μm.

1.25 to 1.42 μm. Especially, at 1.31-μm wavelength, the IL is 0.93 dB, which is only slightly higher than the mode absorption loss $\alpha_m(N_1) = 0.86$ dB. This indicates an efficient coupling from the TE_0 mode of the Si strip waveguide to the TM_0 mode of the slot-waveguide modulator for the ON state. The corresponding ER here is 11.75 dB. Fig. 7 shows the light propagation from the front end to the back end (including the polarization rotators on both sides) at 1.31 μm with carrier concentrations of N_1 and N_4, respectively. The normalized transmission at the output are 81.4 $\%$ in Fig. 7(a) and 5.4 $\%$ in Fig. 7(b).

B. Evanescent-Coupled Scheme

In the previous section, by incorporating polarization rotators, the slot-waveguide modulator was connected with TE-loaded Si strip waveguides and other passive/active components that operate for TE-polarized light. Alternatively, the slot-waveguide modulator can be evanescently coupled to TM-loaded Si strip waveguides, therefore we investigate such a structure in this section.

As shown in Fig. 8, the ITO-based modulator layers are positioned on top of a Si strip waveguide (220 nm thick and 400 nm wide). Compared with butt coupling, evanescent coupling is less efficient, however, it simplifies the fabrication. Fig. 9(a) shows the performance of the slot-waveguide modulator with 10-nm thick SiO_2 buffers as a function of the device length (L_m) at the wavelength of 1.31 μm. In this case, the carrier concentration is tuned from N_1 to N_4. When the device length increases, the ER increases gradually while the IL experiences periodic variation. To achieve a high ER and a low IL, we set L_m = 1.5 μm. For a wavelength of 1.31 μm, the ER and IL are 10.1 and 1.5 dB, respectively. The performance of the modulator with L_m = 1.5 μm over a broad wavelength range is shown in Fig. 9(b). The ER is greater than 6.0 dB while the IL is less than 1.7 dB for a wavelength ranging from 1.25 to 1.39 μm.

V. Conclusion

In this paper, a compact broadband modulator design based on engineered ENZ ITO materials has been presented. By assuming electrically tunable permittivity of the active ITO layer between the states with carrier concentrations

of $N_1 = 4.33 \times 10^{20}\,\mathrm{cm}^{-3}$, $N_2 = 6.67 \times 10^{20}\,\mathrm{cm}^{-3}$, $N_3 = 8.31 \times 10^{20}\,\mathrm{cm}^{-3}$ and $N_4 = 9.58 \times 10^{20}\,\mathrm{cm}^{-3}$, the optical loss of the proposed slot-waveguide modulator has been modulated with high efficiency. We have also discussed two methods that integrate our modulator with Si Strip waveguides. In the first method, using a butt-coupled scheme with a 1.0-μm device length, our modulator has demonstrated a high ER above 6.0 dB and an IL below 1.3 dB for a wavelength ranging from 1.25 to 1.42 μm. By adjusting the carrier concentration, the broadband modulation has been demonstrated when the wavelength is around 1.55 μm. In the second method (i.e., the evanescent coupling scheme with a 1.5-μm device length), an ER greater than 6.0 dB and an IL less than 1.7 dB have been achieved for a wavelength ranging from 1.25 to 1.39 μm.

REFERENCES

[1] D. A. B. Miller, “Device requirements for optical interconnects to silicon chips,” *Proc. IEEE.*, vol. 97, no. 7, pp. 1169–1185, Jul. 2009.

[2] J. Klamkin *et al.*, “A 100-Gb/s noncoherent silicon receiver for PDMDBPSK/DQPSK signals,” *Opt. Exp.*, vol. 22, no. 2, pp. 2150–2158, 2014.

[3] M. Asghari and A. Krishnamoorthy, “Silicon photonics: Energy-efficient communication,” *Nature Photon.*, vol. 5, pp. 268–270, 2011.

[4] W. M. Green, M. J. Rooks, L. Sekaric, and Y. A. Vlasov, “Ultra-compact, low RF power, 10 Gb/s silicon Mach-Zehnder modulator,” *Opt. Exp.*, vol. 15, no. 25, pp. 17-106–17-113, 2007.

[5] Q. Xu, S. Manipatruni, B. Schmidt, J. Shakya, and M. Lipson, “12.5 Gbit/s carrier-injection-based silicon microring silicon modulators,” *Opt. Exp.*, vol. 15, no. 2, pp. 430–436, 2007.

[6] Y. Kuo *et al.*, “Quantum-confined stark effect in Ge/SiGe quantum wells on Si for optical modulators,” *IEEE J. Sel. Topics Quantum Electron.*, vol. 12, no. 6, pp. 1503–1513, Nov/Dec. 2006.

[7] J. Liu *et al.*, “Waveguide-integrated, ultralow-energy GeSi electro-absorption modulators,” *Nature Photon.*, vol. 2, no. 7, pp. 433–437, 2008.

[8] Z. Lu, W. Zhao, and K. Shi, “Ultracompact electroabsorption modulators based on tunable epsilon-near-zero slot waveguides,” *IEEE Photon. J.*, vol. 4, no. 3, pp. 735–740, Jun. 2012.

[9] V. Babicheva *et al.*, “Towards CMOS-compatible nanophotonics: Ultra-compact modulators using alternative plasmonic materials,” *Opt. Exp.*, vol. 21, no. 22, pp. 27-326–27-336, 2013.

[10] P. West *et al.*, “Searching for better plasmonic materials,” *Laser Phton. Rev.*, vol. 4, no. 6, pp. 795–808, 2010.

[11] G. Naik, J. Kim, and A. Boltasseva, “Oxides and nitrides as alternative plasmonic materials in the optical range,” *Opt. Mater. Exp.*, vol. 1, no. 6, pp. 1090–1099, 2011.

[12] A. Melikyan *et al.*, “Surface plasmon polariton absorption modulator,” *Opt. Exp.*, vol. 19, no. 9, pp. 8855–8869, 2013.

[13] V. Sorger, N. Lanzillotti-Kimura, R. Ma, and X. Zhang, “Ultracompact silicon nanophotonic modulator with broadband response,” *Nanophotonics*, vol. 1, no. 1, pp. 17–22, 2012.

[14] C. Ye, S. Khan, Z. Li, E. Simsek, and V. Sorger, “λ-size ITO and graphene-based electro-optic modulators on SOI,” *IEEE J. Sel. Topics Quantum Electron.*, vol. 20, no. 4, art. no. 3400310 Jul/Aug. 2014.

[15] A. Vasudev, J. Kang, J. Park, X. Liu, and M. Brongersma, “Electrooptical modulation of a silicon waveguide with an epsilon-near-zero material,” *Opt. Exp.*, vol. 21, no. 22, pp. 26-387–26-397, 2013.

[16] E. Feigenbaum, K. Diest, and H. A. Atwater, “Unity-order index change in transparent conducting oxides at visible frequencies,” *Nano. Lett.*, vol. 10, pp. 2111–2116, 2010.

[17] A. Capretti, Y. Wang, N. Engheta, and L. D. Negro, “Tailored optical nonlinearity in Si-compatible epsilon-near-zero materials,” *Nature Mater.*, submitted for publication.

[18] H. Zhao, P. Contu, and J. Klamkin, “Silicon nanophotonic waveguide modulator with graphene active medium,” presented at the Integrated Photonic Research., San Diego, CA, USA, 2014, Paper JM3B.4.

[19] J. Zhang, M. Yu, G. Lo, and D. Kwong, “Silicon-waveguide-based mode evolution polarization rotator,” *IEEE J. Sel. Topics Quantum Electron*, vol. 16, no. 1, pp. 53–60, Jan/Feb. 2010.

Hongwei Zhao received the undergraduate degree with a B.Eng. degree in electronics from the Huazhong University of Science and Technology, Wuhan, China, in 2008, and the M.S. degree from the Institute of Semiconductors, Chinese Academy of Sciences, Beijing, China, in 2011. She is currently a Research Assistant in the Integrated Photonics Lab at the Department of the Electrical and Computer Engineering, Boston University, Boston, MA, USA. Her research interests include the design and fabrication of the nanophotonic waveguide modulators.

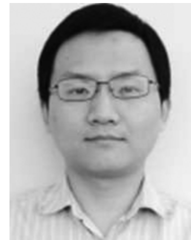

Yu Wang received the B.Eng. degree in optoelectronic information from the HuaZhong University of Science and Technology, WuHan, China, in 2010, and the M.S. degree in electro-optics from the University of Dayton, Dayton, OH, USA, in 2012. He is currently working toward the Ph.D. degree in electrical engineering at the Department of Electrical and Computer Engineering and Photonics Center, Boston University, Boston, MA, USA. His research interests include fabrication, simulation, structural, optical, and electrical characterization of optoelectronic material and nanoscale photonic structures based on transparent conductive oxides for light emission devices.

Antonio Capretti received the Laurea and Laurea Specialistica (B.S. and M.S. degrees) cum laude in electronic engineering in 2007 and 2009, respectively, and the Ph.D. degree in electrical engineering with a thesis on nonlinear plasmonics, in 2003, all from the University of Naples Federico II, Napoli, Italy. He was a Visiting Researcher at the Department of Electrical and Computer Engineering, Boston University, Boston, MA, USA, from 2011 to 2012. He is currently a Postdoctoral Associate at the Department of Electrical and Computer Engineering, Boston University. His research interests include nano-optics and photonics, superconductivity, and computational electromagnetism.

Luca Dal Negro received the Laurea degree in physics, cum laude, and the Ph.D. degree in semiconductor physics from the University of Trento, Trento, Italy, in 1999 and 2003, respectively. After his Ph.D. degree in 2003, he joined the Massachusetts Institute of Technology as a Postdoctoral Research Associate. Since January 2006, he has been a Faculty Member of the Department of Electrical and Computer Engineering and the Photonics Center at Boston University, Boston, MA, USA, where he is currently a tenured Associate Professor. His main research interests include light–matter interaction in aperiodic media, nanophotonics, complex plasmonic nanostructures, and computational electrodynamics. He received the 2009 National Science Foundation CAREER Award, published more than 180 technical articles, and has been an Invited Speaker at numerous international conferences and symposia.

Jonathan Klamkin (SM'14) received the B.S. degree in electrical and computer engineering (ECE) from Cornell University, Ithaca, NY, USA, in 2002, and the M.S. degree in ECE and the Ph.D. degree in materials from the University of California Santa Barbara, CA, USA, in 2004 and 2008, respectively. From 2008 to 2011, he was a Member of the Technical Staff in the Electro-Optical Materials and Devices Group at MIT Lincoln Laboratory. From 2011 to 2013, he was an Assistant Professor at the Institute of Communication, Information and Perception Technologies, Scuola Superiore Sant'Anna, Pisa, Italy, where he received the Erasmus Mundus scholarship and a Marie Curie fellowship, and served as the Director of the Integrated Photonic Technologies Center. In 2013, he joined Boston University (BU), Boston, MA, USA, as an Assistant Professor in ECE and Materials Science and Engineering. He is also affiliated with the BU Photonics Center and leads the Integrated Photonics Group. He has served on the Technical Program Committee for the Microwave Photonics Conference, the IEEE Photonics Conference, Photonics in Switching, the Optical Fiber Communication Conference, Integrated Photonics Research, and Silicon and Nanophotonics. He has authored or coauthored 90 papers on photonic integrated circuits, silicon photonics, nanophotonics, microwave photonics, coherent receivers, high-power photodiodes, optical modulators, high-power lasers, widely tunable lasers, and semiconductor optical amplifiers. He received Best Paper Awards at the 2006 Conference on Optoelectronic and Microelectronic Materials and Devices and the 2007 Microwave Photonics Conference, and received a NASA Early Career Faculty Research Grant. He is a Member of the OSA.